Center for Turbulence Research
Annual Research Briefs 1994

Lewis number and Damköhler number effects in vortex-flame interactions

By J.-M. Samaniego

1. Motivation and objectives

Premixed flames are encountered in numerous practical configurations, and a better knowledge of the fundamental mechanisms controlling their propagation is needed to help model their behavior. In practical devices, premixed flames generally propagate into a turbulent stream of reactants, and their structure and local flame speed are modified. Although some recent studies demonstrate the persistence of laminar flame structures under highly turbulent conditions (Poinsot *et al.* 1991, Furukawa *et al.* 1993), the structure of turbulent premixed flames, either as a flamelet or thickened flame, is still a matter of debate. Hence, the development of turbulent combustion diagrams is an ongoing effort (Borghi 1988, Poinsot *et al.* 1991). However, despite uncertainties concerning the actual structure of premixed flames in real combustion devices, studies of the propagation properties of a laminar flame in turbulent flow conditions contribute to a better understanding of turbulent premixed flames. In such flows, premixed flames experience stretch, strain, curvature, and unsteadiness, and are subject to various effects depending on the thermodiffusive properties of the mixture (Lewis number), adiabaticity (heat losses), and detailed kinetics (Clavin 1985, Borghi 1988, Law 1988, Clavin 1994).

In order to study these effects in detail, a combined experimental-numerical study of the interaction of a two-dimensional vortex pair with a plane premixed laminar flame has been carried out. The selected geometry is two-dimensional in order to allow for the use of quantitative line-of-sight measurement techniques and for comparisons with two-dimensional direct numerical simulations. The experiment is used to identify possible effects of the Lewis number and of radiative heat losses, and direct numerical simulations reproducing the experimental conditions are used to investigate the role of the Lewis number, of heat losses, and of multi-step kinetics. The heat losses considered in this study are essentially radiative losses from the burnt gases and do not include conductive losses to the walls.

This report presents the final results of this study of vortex-flame interactions. The main result is the creation of experimental data sets of vortex-flame interactions, which demonstrate the importance of the Lewis and Damköhler numbers to the flame and which allow for comparison with direct numerical simulations. In turn, the comparison between experimental and numerical results, presented in Mantel 1994, shows that the Lewis number effects and complex chemistry play significant roles, which can be reproduced using a two-step reaction mechanism.

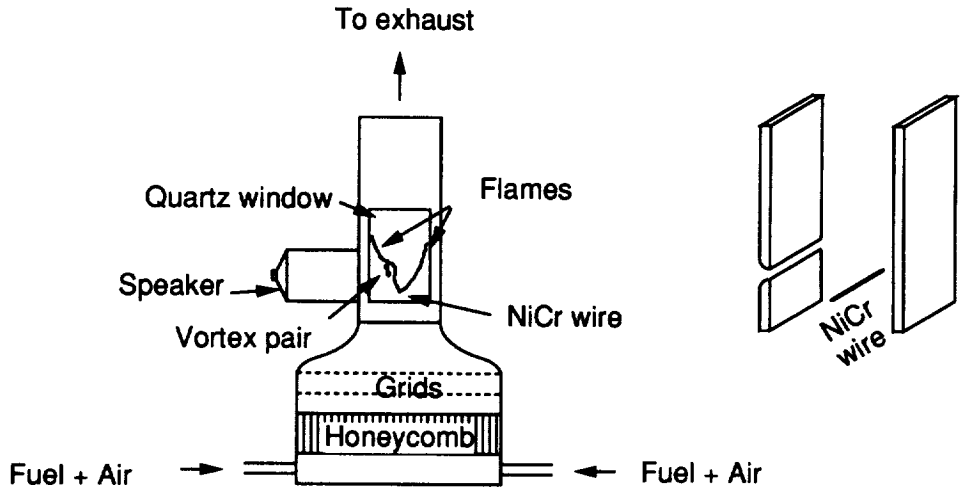

FIGURE 1. Schematic view of the facility

2. Accomplishments

2.1 Experimental details

An experimental facility with a two-dimensional flow has been developed and has been described in the last issue of the Annual Research Briefs, where details about the vortex generation and flame stabilization are reported (Samaniego 1993). The two-dimensionality of the flow field is an important feature of this study since it allows for comparison with two-dimensional direct numerical simulations of vortex-flame interactions. The choice of a two-dimensional flow field is dictated by the necessity of providing numerous quantitative experimental and numerical data in the simplest though relevant flow configuration by the use of line-of-sight CO_2^* emission imaging as a quantitative measurement of the heat release rate, and by limitations of current computer capabilities that would render three-dimensional calculations with multi-step kinetics too expensive.

The test section comprises a vertical duct, with a square cross-section of 63.5 $\times$ 63.5 mm, equipped with quartz windows for optical access (see Fig. 1). Mixtures of fuel and oxidizer are fed into the test section through a contoured converging nozzle. Different fuel and oxidizer mixtures are used to investigate the effect of the Lewis number. The Lewis number is determined using mixture-averaged properties (Strehlow 1979, Williams 1985). Five fuel-lean mixtures were investigated: $\phi = 0.55$ CH_4/Air ($Le = 0.96$), $\phi = 0.46$ C_2H_4/Air ($Le = 1.24$), $\phi = 0.51$ C_3H_8/Air ($Le = 1.60$), $\phi = 0.61$ $CH_4/O_2/CO_2/Ar$ ($Le = 0.80$), and $\phi = 0.61$ $CH_4/O_2/CO_2/He$ ($Le = 1.54$). The flame is stabilized on a heated Nichrome wire of 0.5 mm diameter, resulting in a V-shaped flame.

Several parameters describing the vortex pair and the flame control the interaction between the vortex and the flame. The vortex parameters, determined from smoke

Table 1. Vortex parameters

type of vortex	$s\ (cm)$	$V_D\ (cm/s)$	$R\ (cm)$	$\tau_r\ (ms)$
Slow	0.85	135.	10.0	4.15
Medium	0.60	350.	4.0	2.07
Fast	0.60	600.	7.4	1.09

Table 2. Flame parameters

Mixture	ϕ	T_{ad} (K)	α_m (deg)	S_L (cm/s)	δ_L (cm)	Le	HL $\times 10^{-3}$
CH_4/Air	0.55	1567	13	9.5	0.022	0.94	0.55
C_2H_4/Air	0.46	1515		9	0.022	1.25	
C_3H_8/Air	0.51	1530	15	9	0.020	1.60	0.40
$CH_4/O_2/CO_2/He$	0.61	1643		13.8	0.033	1.54	1.10
$CH_4/O_2/CO_2/Ar$	0.61	1615		6.7	0.024	0.82	2.50

visualization experiments, are: the distance between the vortex centers, s, the vortex pair self-induced velocity, V_D, and the radius of curvature of the trajectory, R. The flame parameters are: the mean flame angle, α_m, the flame speed, S_L, the flame thickness, δ_L, the Lewis number, Le, and a heat loss coefficient, HL, which is defined as the ratio of the radiative loss in the reaction zone to the chemical energy release. They depend on the mixture composition (fuel, diluent) and on the bulk flow velocity, V_0. In the present study, $V_0 = 0.35\ m/s$. The vortex and flame parameters are reported in Tables 1 and 2. Details on the determination of these parameters can be found in Samaniego *et al.* 1994a.

Line-of-sight CO_2^* emission imaging, using an intensified CCD camera, is performed to obtain heat release rate fields. Each image is digitized in a 184 × 240 8-bits pixel array (a pixel corresponds to a field of vue of 0.364 × 0.364 mm). The light intensifier is used as a fast shutter in order to freeze the flow field. The exposure time is 250 μs, resulting in a spatial resolution of 1.5 mm in the worst case. A timing circuit allows the triggering of the intensifier at selected instants during the interaction. For each value of the time delay, ten to fifty realizations are averaged in order to improve the signal-to-noise ratio. Images are corrected for background noise and pixel-to-pixel variations. After correction, the uncertainty on the pixel

value is ± 2 % of the maximum value in the worst case.

2.2 Determination of the heat release rate

The rate of heat release is an important flame quantity which controls its propagation, and its monitoring provides insight into the respective effects of the Lewis number, radiative losses, and complex chemistry. The choice for studying this quantity is made for two reasons: first, it can be determined experimentally by measuring the flame chemiluminescence; second, this quantity is predicted by most combustion models and can therefore be used for their validation by comparison with experimental data.

Chemiluminescence refers to light spontaneously emitted by electronically excited molecules as they decay to their ground state. In hydrocarbon flames such as those investigated here, flame chemiluminescence occurs in the UV and visible range of the spectrum and is due principally to four emitters: CH^*, C_2^*, OH^*, and CO_2^*. These electronically-excited molecules have different emission spectra. The first three emitters have band-structured emission spectra which correspond to specific electronic transitions (CH^* peak at 431.5 nm corresponding to the $A^2\Delta \rightarrow X^2\Pi$ transition, C_2^* peak at 516.6 nm corresponding to the $A^3\Pi - X^3\Pi$ transition, OH^* peak at 306.4 nm corresponding to the $^2\Sigma^+ \rightarrow^2 \Pi$ transition Gaydon 1974), while CO_2^* has a broadband emission spectrum extending from 250 to 800 nm (Myers & Bartle 1967).

Recently, Samaniego *et al.* 1994b, after showing that CO_2^* is the main emitter in fuel-lean flames, have successfully correlated the CO_2^* emission intensity and the rate of heat release for a $\phi = 0.55$ CH_4/Air flame based on complex chemistry calculations of strained flames. The resulting correlation takes the form:

$$\frac{\mathcal{Q}}{\mathcal{Q}_0} = \left(\frac{\mathcal{I}}{\mathcal{I}_0}\right)^{0.37} \tag{1}$$

where $\mathcal{Q}$ is the integral of the heat release rate, Q, across the flame front, i.e.:

$$\mathcal{Q} = \int_{-\infty}^{+\infty} Q dx \quad ,$$

$\mathcal{I}$ is the CO_2^* emission intensity integrated across the flame front, i.e.:

$$\mathcal{I} = \int_{-\infty}^{+\infty} I dx \quad ,$$

and the subscript 0 refers to the unstrained premixed laminar CH_4/Air flame ($\phi = 0.55$).

It was shown that expression (1) is not affected by unsteadiness and can be used to determine the heat release rate in situations where strain-rate is the only significant parameter controlling the flame evolution. As is discussed later, it is the case in the present study of vortex-flame interactions since the effect of curvature, which is not accounted for in Eq. (1), can be neglected.

FIGURE 2. Dithered images of CO_2^* emission of a $\phi = 0.51$ propane-air flame. *left*: $t = 0$, *center*: $t = 17\ ms$, *right*: $t = 19\ ms$.

However, Eq. (1) is only strictly valid for the $\phi = 0.55\ CH_4/Air$ flame, and new correlations should be sought for other mixture compositions (i.e. different fuel, different diluent).

2.3 CO_2^* emission imaging

Instantaneous images of CO_2^* emission from the flame were obtained using an intensified Amperex CCD camera equipped with a NIKON glass lens ($f = 105\ mm$, $f/1.2$) and a band-pass filter BG39 with cut-off wavelengths at 340 and 700 nm. This filter is used to reject near-infrared emission (700-1200 nm) from the burnt gases originating from H_2O excited molecules (Gaydon 1974).

Fig. 2 shows a sequence of three flame emission images of a C_3H_8/Air flame at $\phi = 0.51$ taken during a vortex-flame interaction. The parameters of this interaction are: $s = 6.0\ mm$, $V_D = 3.5\ m/s$, $R = 40\ mm$, $S_L \simeq 0.10\ m/s$, $\delta_L \simeq 1.0\ mm$, $Le = 1.60$, $\alpha \simeq 15\ degrees$.

The first image shows the unperturbed flame fronts. The next two images in Fig. 2 are taken respectively at $t = 17\ ms$ and $t = 19\ ms$. Three regions in the distorted portion of the flame can be identified: 1) a region of extensive strain-rate and negative curvature, located just ahead of the vortex pair. In this region, strain-rate effects are predominant, and Eq. (1) can be confidently used to infer the heat release rate; 2) & 3) regions of high positive curvature, located above and under region 1. In these regions, curvature may play a significant role, and the validity of Eq. (1) remains to be evaluated. Therefore, quantitative comparisons between experimental and numerical data should be restricted to the regions of high strain.

For this purpose, $\mathcal{I}_{min}$ is defined as the minimum value of $\mathcal{I}(\sigma)$, where $\mathcal{I}(\sigma)$ is defined as the integral of the CO_2^* emission, I, across the reaction zone, at the

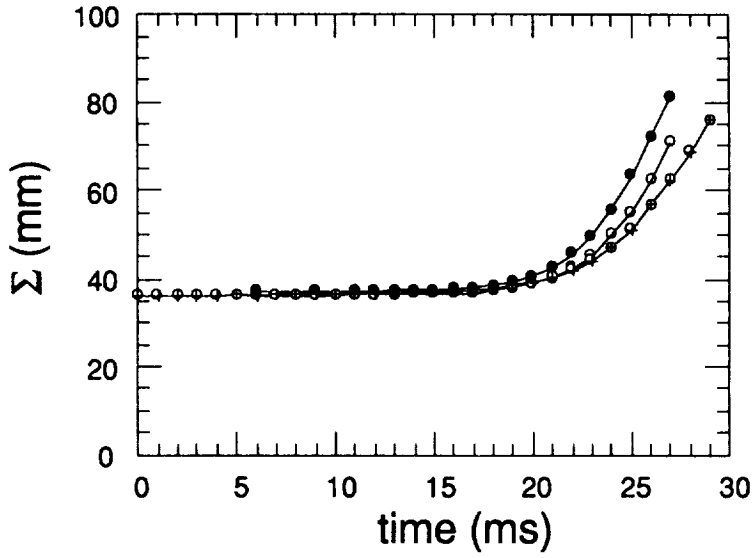

FIGURE 3. Slow vortex. Evolution of Σ. o : $Le = 0.94$, ⊕ : $Le = 1.25$, • : $Le = 1.60$ (see Table 2).

location σ along the flame front, i.e.:

$$\mathcal{I}(\sigma) = \int_{\sigma^\perp} I d\sigma^\perp ,$$

where $\perp$ indicates that integration is performed along a normal-to-the-flame front, and

$$\mathcal{I}_{min} = \min_{\sigma} \mathcal{I}(\sigma)$$

In all cases, $\mathcal{I}_{min}$ occurs in front of the vortex pair in the region of high extensive strain. The corresponding minimum heat release rate, $\mathcal{Q}_{min}$ is obtained from $\mathcal{I}_{min}$ using expression (1).

2.4 Effect of the Lewis number

The theory of stretched flames predicts that the behavior of strained flames is controlled by the Lewis number, Le (Clavin 1985, Law 1988). For positively stretched flames such as in vortex-flame interactions, the burning rate should increase for $Le < 1$ flames while it should decrease for $Le > 1$ flames. This prediction is checked by monitoring the evolution of $\mathcal{I}_{min}$, during vortex-flame interactions, between the slow vortex and all flames (each flame corresponds to a different Lewis number - see Tables 1 and 2).

It is first verified that all flames undergo the same stretch history. Fig. 3 shows the evolution of the flame surface area, Σ, during vortex-flame interactions with the

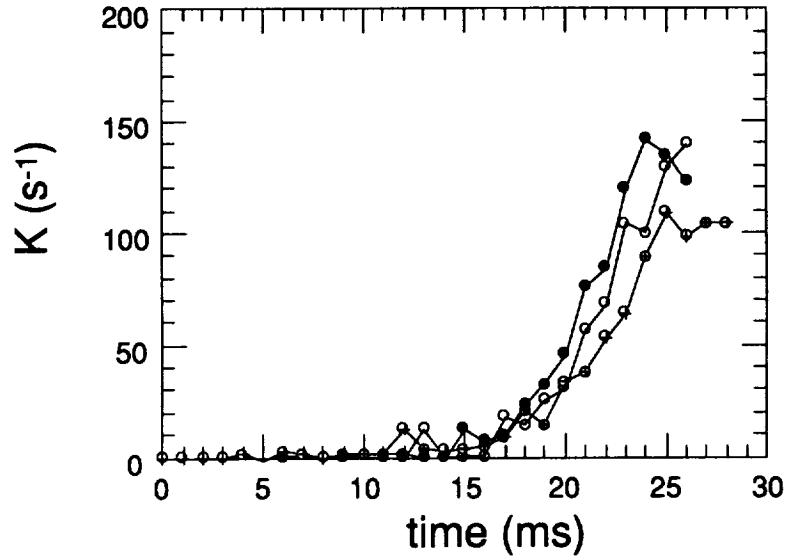

FIGURE 4. Slow vortex. Evolution of K_{mean}. ○ : $Le = 0.94$, ⊕ : $Le = 1.25$, ● : $Le = 1.60$ (see Table 2).

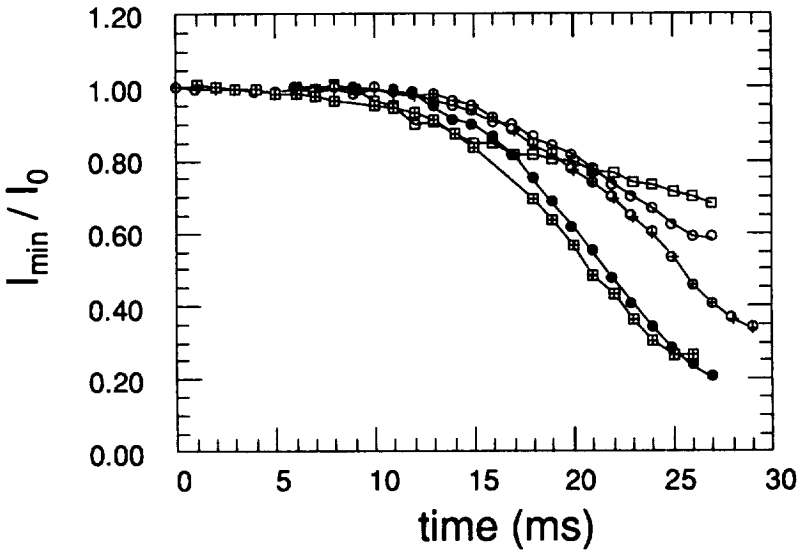

FIGURE 5. Slow vortex. Evolution of $\mathcal{I}_{min}$ for all investigated flames (see Table 2). □ : $Le = 0.82$, ○ : $Le = 0.94$, ⊕ : $Le = 1.25$, ⊞ : $Le = 1.54$, ● : $Le = 1.60$.

slow vortex pair for all flames. The flame surface area, Σ, starts increasing after t = 15 ms. A mean stretch-rate, K_{mean}, can be derived:

$$K_{mean} = \frac{1}{\Sigma}\frac{d\Sigma}{dt}$$

K_{mean} also starts increasing after $t = 15\ ms$ and reaches about 100 to 150 s^{-1} at $t = 25\ ms$ (see Fig. 4). All flames experience the same overall stretch history which allows us to interpret possible differences between these flames in terms of a Lewis number effect.

The effect of the Lewis number on the evolution of $\mathcal{I}_{min}$ for all flames is shown in Fig. 5. In all cases, $\mathcal{I}_{min}$ starts at the value of the unperturbed laminar flame and then decreases under the action of the vortex pair. It can be noticed that the decrease is more pronounced for higher Lewis number flames. This is better demonstrated in Fig. 6 where the maximum slope of the evolution of $\mathcal{I}_{min}$, b, is plotted as a function of the Lewis number, where the slope b decreases with increasing Lewis number.

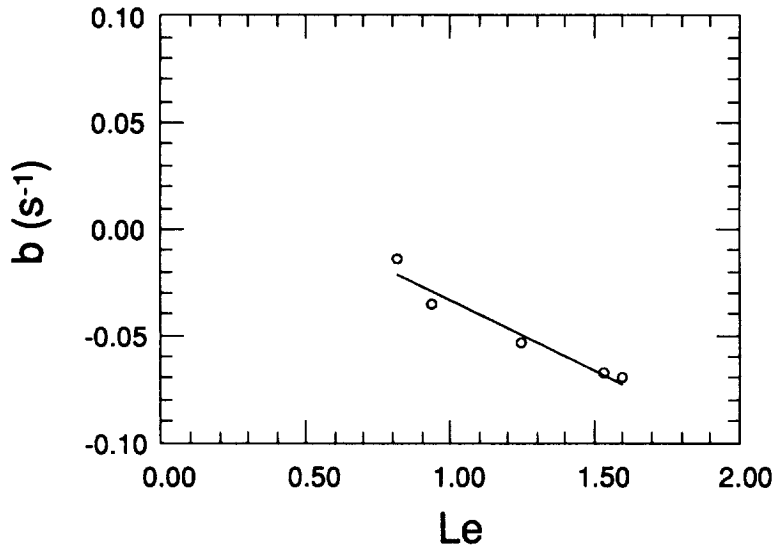

FIGURE 6. Slow vortex. Correlation between the rate of variation of $\mathcal{I}_{min}$ (b), with the Lewis number (Le).

These results are only in partial agreement with the asymptotic theory: higher Lewis numbers lead to flames that are weaker when strained. However, the theory predicts that the burning rate of $Le < 1$ flames increases with strain, but we observe a decrease of $\mathcal{I}_{min}$ for all flames, including the $Le = 0.8$ flame. This may be attributed to various causes: unsteady effects (see section 2.5, theory limited to low stretch-rates, complex chemistry effects (see DNS).

2.5 Effect of the Damköhler number

Unsteadiness is an important factor in these vortex-flame interactions which is not accounted for in the theory of stretched flames. Unsteadiness is quantified by the

Damköhler number, defined as the ratio of a mechanical time, τ_m, over a chemical time, τ_c, i.e.

$$Da = \frac{\tau_m}{\tau_c}$$

In this study, τ_m is the characteristic time of evolution of the flame surface area and τ_c is the residence time through the flame, i.e. $\tau_c = \delta_L/S_L$. τ_m is defined by the time for Σ to increase from $1.25 \times \Sigma_0$ to $2.00 \times \Sigma_0$ where Σ_0 is the unperturbed value.

2.5.1 Observations

The effect of the Damköhler number is determined by investigating the evolution of the overall heat release rate Q_{tot}, and the minimum heat release rate $\mathcal{Q}_{min}$. Q_{tot} is defined as the total heat released by the flame of surface area Σ and is computed as:

$$Q_{tot} = \int_{\Sigma} \mathcal{Q}(\sigma) d\sigma \tag{2}$$

Fig. 7 shows the evolution of Σ, Q_{tot}, and $\mathcal{Q}_{min}$ for the $\phi = 0.55$ CH_4/Air flame during its interaction with the slow, medium, and fast vortex pairs (see Tables 1 and 2). These interactions are characterized by $Da = 1.80$, 0.90, and 0.47, respectively. Lower values of Da can be interpreted as higher stretch rates. Each set of curves corresponds to a different Damköhler number. In all cases Q_{tot} lags Σ. This is consistent with the fact that $\mathcal{Q}_{min}$ decreases due to flame stretch. Indeed, if $\mathcal{Q}_(\sigma)$ were constant along the flame front during vortex-flame interactions, Q_{tot} would be proportional to Σ (see expression (2)). Hence, the non-linearity of the relationship between Q_{tot} and Σ is a consequence of stretching due to the vortex pair.

In order to stress the effect of Da, Σ and Q_{tot} are plotted in a non-dimensional time-frame, t^+, where time is non-dimensionalized by τ_m, and the origin corresponds to the time at which $\Sigma = 1.25 \times \Sigma_0$ (Fig. 8). The evolution of Σ is independent of the Damköhler number. This follows mainly from the non-dimensionalization procedure which imposes $\Sigma(t^+ = 0) = 1.25 \times \Sigma_0$ and $\Sigma(t^+ = 1) = 2.00 \times \Sigma_0$. The evolution of Q_{tot} shows a certain similarity in all three cases: Q_{tot} starts decreasing, reaches a minimum value, and finally increases at a pace comparable with the evolution of Σ. One can notice that the minimum value reached by Q_{tot} decreases with decreasing Da and that higher values of Da lead to less non-linearity between Q_{tot} and Σ. Third, the decrease $\mathcal{Q}_{min}$ is less pronounced for higher values of Da. These observations display trends that are in agreement with the idealized infinitely fast chemistry limit, or $Da \rightarrow \infty$, where the internal structure of the flame is not affected by the flow. In this case, $\mathcal{Q}(\sigma)$ would be constant, and Q_{tot} would be proportional to Σ. Indeed, as shown in Fig. 8, Q_{tot} converges towards Σ as Da increases.

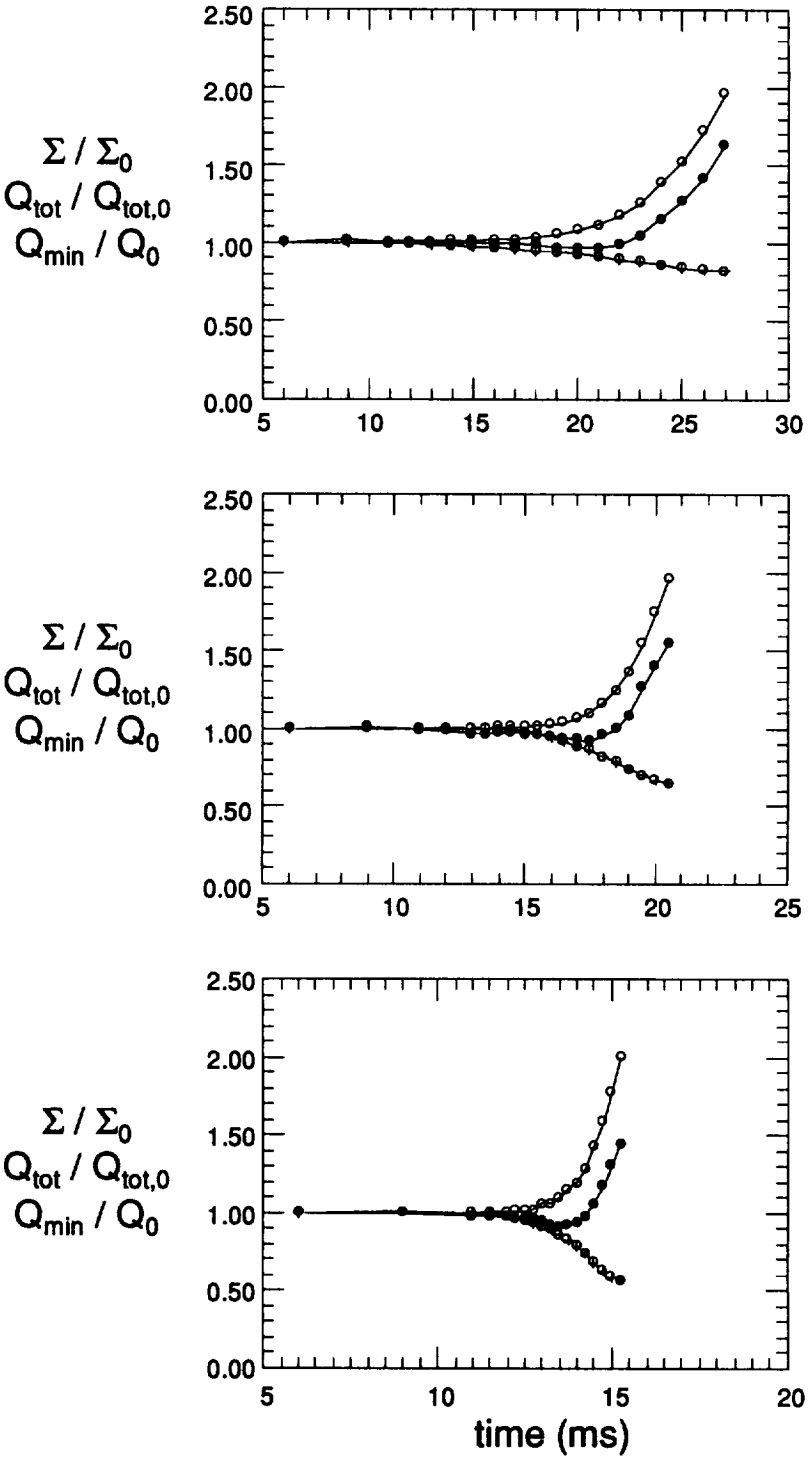

FIGURE 7. CH_4/Air flame ($\phi = 0.55$). Evolution of Σ/Σ_0 ($\circ$), $Q_{tot}/Q_{tot,0}$ ($\bullet$), and Q_{min}/Q_0 ($\circledcirc$). *Top*: slow vortex ($Da = 1.80$), *center*: medium vortex ($Da = 0.90$), *bottom*: fast vortex ($Da = 0.47$).

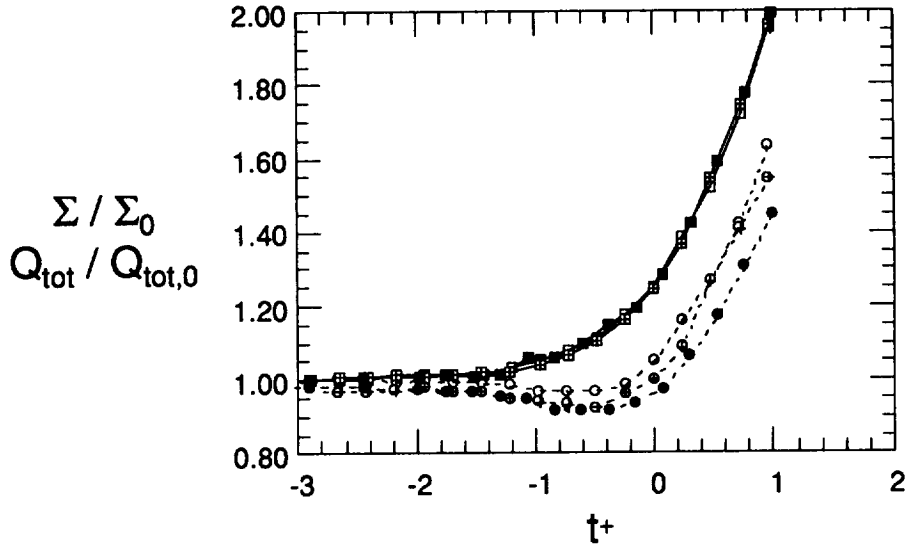

FIGURE 8. CH_4/Air flame ($\phi = 0.55$). Effect of Da on the relationship between Σ/Σ_0 and $Q_{tot}/Q_{tot,0}$. $Q_{tot}/Q_{tot,0} \rightarrow$ ○ : $Da = 1.80$, ⊕ : $Da = 0.90$, ● : $Da = 0.47$. $\Sigma/\Sigma_0 \rightarrow$ □ : $Da = 1.80$, ⊞ : $Da = 0.90$, ■ : $Da = 0.47$.

2.5.2 Stretching-relaxation mechanism

For finite values of Da, unsteadiness, in addition to stretch, plays an important role. This can be seen in recent studies of unsteady strained laminar flames (see for example Darabiha 1992, Egolfopoulos 1994). A simple stretching-relaxation model accounting for unsteadiness may be derived. The main assumption is that two mechanisms are important: unsteady strain which tends to thin the flame without modifying the internal flame structure, and the diffusion-reaction process which relaxes the flame back to an unstrained laminar structure. Effects of curvature are neglected. Both mechanisms contribute to dQ/dt. They can be modeled by two additive effects: a term of the form $-KQ$ due to stretch, and a relaxation term of the form $(Q_0 - Q)/\tau_r$, where τ_r is a relaxation time. The term due to strain-rate can be justified by two arguments: 1) curvature being neglected, stretch is equal to the strain-rate tangential to the flame front, and we have $K = a_T$; 2) the flame front undergoes a compression $-a_T$ along its normal. Therefore the flame front is compressed at a rate $-K$ along its normal, and the rate of change of Q due to stretch is equal to $-K\dot{Q}$. The second term is an *ad-hoc* representation of the diffusion-reaction process using a linear relaxation model and is justified by the fact that the Q must relax to Q_0 in the absence of stretch (actually, different forms for the relaxation term could be used since there is no real justification for a linear relaxation process). Therefore, an evolution equation for Q may be derived:

$$\frac{dQ}{dt} = -KQ + \frac{Q_0 - Q}{\tau_r} \tag{3}$$

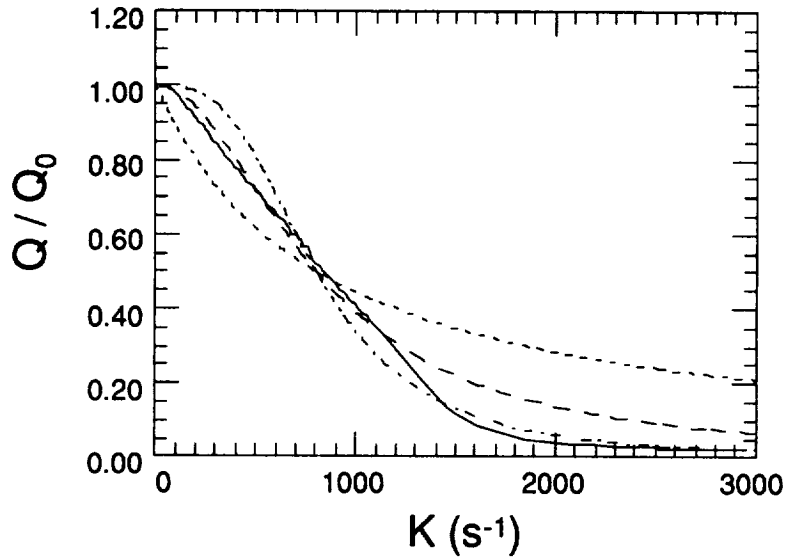

FIGURE 9. Evolution of Q/Q_0 with strain-rate for a steady strained CH_4/Air flame ($\phi = 0.55$). Comparison between model predictions (with $\tau_r = 1.25\ ms$) and complex chemistry calculations. ——— : complex chemistry, ---- : linear relaxation model, — — — : quadratic relaxation model, —·— : cubic relaxation model.

Interestingly enough, in the steady case (i.e. $\frac{dQ}{dt} = 0$), this model yields:

$$\frac{Q}{Q_0} = \frac{1}{1 + K\tau_r}$$

This prediction is compared to the evolution of the relative heat release rate for a strained $\phi = 0.55$ CH_4/Air flame, computed from complex chemistry calculations (Samaniego *et al.* 1994b) (Fig. 9). Other predictions using non-linear relaxation terms are also plotted for comparison (quadratic: $\frac{Q_0}{\tau_r}(1 - Q/Q_0)^{1/2}$, and cubic: $\frac{Q_0}{\tau_r}(1 - Q/Q_0)^{1/3}$). In this case, $\tau_r = 1.25\ ms$ is the same for all three relaxation models and is chosen to best reproduce the evolution of Q/Q_0 predicted by the complex chemistry calculations. It appears that all relaxation models predict correctly the qualitative behavior of Q/Q_0 and that quadratic relaxation provides the best quantitative agreement. In the following, the linear relaxation model, although imperfect, is used to further investigate the relationship between Q_{tot} and Σ.

Eq. (3) may be integrated over Σ using a transport theorem which accounts for the fact that Σ also changes in time (see Candel & Poinsot 1990). One obtains, after proper non-dimensionalization:

$$\frac{C}{Da}\frac{dQ^+_{tot}}{dt^+} + Q^+_{tot} = \Sigma^+ \tag{4}$$

where $t^+ = t/\tau_m$, $C = \tau_r/\tau_c$ is a constant, $Q^+_{tot} = Q_{tot}/Q_{tot_0}$, and $\Sigma^+ = \Sigma/\Sigma_0$.

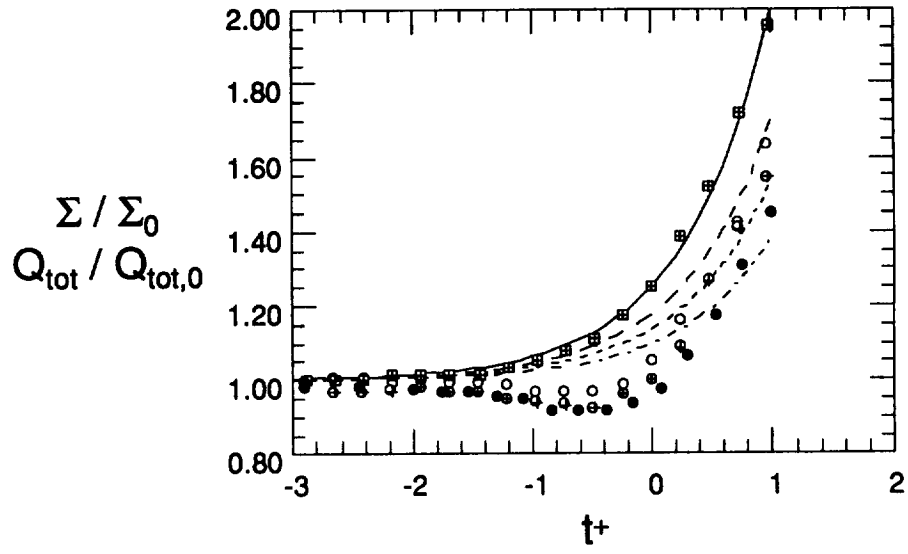

FIGURE 10. Evolution of $Q_{tot}/Q_{tot,0}$ during vortex-flame interactions. Comparison between the linear model ($\tau_r = 1.25\ ms$) and measurements. Model (Eqs. 5 and 6) → ——— : Σ^+, – – – : Q^+_{tot} for $Da = 1.80$, - - - - : Q^+_{tot} for $Da = 0.90$, —·— : Q^+_{tot} for $Da = 0.47$. Experiment → ▪ : Σ^+, ○ : Q^+_{tot} for $Da = 1.80$, ⊖ : Q^+_{tot} for $Da = 0.90$, ● : Q^+_{tot} for $Da = 0.47$.

From this expression it can be seen that, in the limit $Da \to \infty$, $Q^+_{tot} = \Sigma^+$ and the total heat release rate is proportional to the flame surface area, and, in the limit $Da \to 0$, $Q^+_{tot} = 1$ and the total heat release rate is constant.

In turn, Eq. (4) can be integrated once the evolution of Σ is known. A convenient analytic expression for Σ^+ is provided by:

$$\Sigma^+ = 1 + 4^{t-1} \tag{5}$$

This formulation mimics the exponential-like growth of Σ^+ in Fig. 8, and satisfies $\Sigma^+(0) = 1.25$ and $\Sigma^+(1) = 2$. Integrating (4) yields:

$$Q^+_{tot} = 1 + \frac{Da}{(Da + C\ln 4)} 4^{t-1} \tag{6}$$

Fig. 10 shows a prediction of the effect of the Damköhler number using these analytic expressions for Σ and Q_{tot}, with $C = 0.25$. Despite some discrepancies, in particular, the inability of the model to reproduce the initial decrease of Q_{tot}, the effect of Da on Q_{tot} is qualitatively well reproduced.

3. Conclusion

This experimental study of vortex-flame interactions has been successfully conducted, and the initial goals of this study have been achieved. The results have

demonstrated the importance of the thermodiffusive diffusive properties (Lewis number) and of unsteadiness (Damköhler number) on the response of the flame. Quantitative comparisons with direct numerical simulations have demonstrated the importance of complex chemistry effects which could be reproduced using a two-step mechanism.

Further experimental studies of vortex-flame interactions could be carried out to elucidate the effect of the flame (heat release) on the vorticity field. Preliminary results show that the vortex pair is significantly altered in the presence of a flame, and this might be due to the baroclinic torque as well as to buoyancy. This study would shed new light upon the interaction between turbulence and heat release, such as possible jump conditions for turbulence statistics through the flame.

Acknowledgements

This study was made in collaboration with Prof. C. T. Bowman of the High Temperature Gasdynamics Laboratory, Stanford, and in conjunction with a numerical study carried out by Dr. T. Mantel (CTR). I would like to express my gratitude to Dr. T. Poinsot (CERFACS, France), instigator of this study, for his encouragements and fruitful conversations. I would also like to thank F. Levy for his invaluable help during the construction of the facility.

Erratum

The author would like to point out two errors that were made in the previous issue of the Annual Research Briefs (Samaniego 1993). First, what he mistakingly referred to as CH^* emission is actually CO_2^* emission. Second, the presumed linear relationship between the so-denominated CH^* emission and reaction rate does not apply. Both these errors were made before the study on CO_2^* emission, which identified CO_2^* as the main emitter in these flames and led to a quantitative (non-linear) relationship between CO_2^* emission and heat release rate (Samaniego *et al.* 1994b).

REFERENCES

BORGHI, R. 1988 Turbulent Combustion Modeling. *Prog. Energy Combust. Sci.* **14,** 245-292.

CANDEL, S. & POINSOT, T. 1990 Flame stretch and the balance equation for the flame area. *Combust. Sci. Tech.* **70,** 1-15.

CLAVIN, P. 1985 Dynamic behavior of premixed flame fronts in laminar and turbulent flows. *Prog. Energy Comb. Sci.* **11,** 1-59.

CLAVIN, P. 1994 Premixed Combustion and Gasdynamics. *Ann. Rev. Fluid Mech.* **26,** 321-352.

DARABIHA, N. 1992 Transient Behavior of Laminar Counterflow Hydrogen-Air Diffusion Flames With Complex Chemistry. *Combust. Sci. Tech.* **86,** 163-181.

EGOLFOPOULOS, F. N. 1994 Dynamics and Structure of Unsteady, Strained, Laminar Premixed Flames. *to appear in the proceedings of the Twenty Fifth Symposium (International) on Combustion,* The Combustion Institute, Pittsburg.

FURUKAWA, J., MARUTA, K., NAKAMURA, T. & HIRANO, T. 1993 Local Reaction Zone Configuration of High intensity Turbulent Premixed Flames. *Combust. Sci. Tech.* **90,** 267-280.

GAYDON, A. G. 1974 *The Spectroscopy of Flames.* Chapman & Hall, London.

LAW, C. K. 1988 Dynamics of Stretched Flames. *Twenty-Second Symposium (International) on Combustion* The Combustion Institute, Pittsburg, 1381-1402.

MANTEL, T. 1994 Fundamental mechanisms in premixed flame propagation via vortex-flame interactions - numerical simulations. *Annual Research Briefs 1994.* Center for Turbulence Research, NASA Ames Research Center and Stanford University.

MYERS, B. F. & BARTLE, E. R. 1967 Shock-Tube Study of the Radiative Processes in Systems Containing Atomic Oxygen and Carbon Monoxide at High Temperature. *J. Chem. Phys.* **47,** 1783-1792.

POINSOT, T., VEYNANTE, D. & CANDEL, S. 1991 Quenching processes and premixed turbulent combustion diagrams. *J. Fluid Mech.* **228,** 561-605.

SAMANIEGO, J.-M. 1993 Stretch-Induced Quenching in Flame-Vortex Interactions. *Annual Research Briefs 1993.* Center for Turbulence Research, NASA Ames/ Stanford University.

SAMANIEGO, J.-M., MANTEL, T. & BOWMAN, C. T. 1994a Fundamental Mechanisms of Premixed Flame Propagation Via Vortex-Flame Interactions. Part 1: Experiment. *In preparation.*

SAMANIEGO, J.-M., EGOLFOPOULOS, F. N. & BOWMAN, C. T. 1994b CO_2^* Chemiluminescence in Premixed Flames. *In preparation.*

STREHLOW, R. A. 1979 *Fundamentals of Combustion.* Robert E. Kreiger Publishing Company, Huntington, New York.

WILLIAMS, F. A. 1985 *Combustion Theory.* The Benjamin/Cummings Publishing Company, Inc., Menlo Park.